AIP Advances

Magnetic phases in superconducting, polycrystalline bulk FeSe samples

Cite as: AIP Advances **11**, 015230 (2021); https://doi.org/10.1063/9.0000167
Submitted: 29 October 2020 . Accepted: 07 December 2020 . Published Online: 12 January 2021

Quentin Nouailhetas, Anjela Koblischka-Veneva, Michael R. Koblischka, Pavan Kumar Naik S., Florian Schäfer, H. Ogino, Christian Motz, Kévin Berger, Bruno Douine, Yassine Slimani, and Essia Hannachi

Magnetic phases in superconducting, polycrystalline bulk FeSe samples

Cite as: AIP Advances 11, 015230 (2021); doi: 10.1063/9.0000167
Presented: 4 November 2020 • Submitted: 29 October 2020 •
Accepted: 7 December 2020 • Published Online: 12 January 2021

Quentin Nouailhetas,[1,2] Anjela Koblischka-Veneva,[1,3] Michael R. Koblischka,[1,3,a)] Pavan Kumar Naik S.,[4,5] Florian Schäfer,[6] H. Ogino,[3,4] Christian Motz,[6] Kévin Berger,[2] Bruno Douine,[2] Yassine Slimani,[7] and Essia Hannachi[8]

AFFILIATIONS

[1]Institute of Experimental Physics, Saarland University, Campus C 6 3, 66123 Saarbrücken, Germany
[2]Groupe de Recherche en Energie Electrique de Nancy (GREEN), Université de Lorraine, 54506 Vandvre-lès-Nancy, France
[3]Shibaura Institute of Technology, 3-7-5 Toyosu, Koto-ku, Tokyo 135-8548, Japan
[4]Research Institute for Advanced Electronics and Photonics, National Institute of Advanced Industrial Science (AIST), 1-1-1 Central 2, Umezono, Tsukuba, Ibaraki 305-8568, Japan
[5]Department of Physics, Tokyo University of Science, 1-3 Kagurazaka, Shinjuku City, Tokyo 162-8601, Japan
[6]Experimentelle Methodik der Werkstoffwissenschaften, Saarland University, Campus D 3 4, 66123 Saarbrücken, Germany
[7]Department of Biophysics, Imam Abdulrahman Bin Faisal University, P.O. Box 1982, Dammam 31441, Saudi Arabia
[8]Laboratory of Physics of Materials - Structures and Properties, Department of Physics, Faculty of Sciences of Bizerte, University of Carthage, 7021 Zarzouna, Tunisia

Note: This paper was presented at the 65th Annual Conference on Magnetism and Magnetic Materials.
[a)]**Author to whom correspondence should be addressed:** m.koblischka@gmail.com and miko@shibaura-it.ac.jp

ABSTRACT

The FeSe compound is the simplest high-temperature superconductor (HTSc) possible, and relatively cheap, not containing any rare-earth material. Although the transition temperature, T_c, is just below 10 K, the upper critical fields are comparable with other HTSc. Preparing FeSe using solid-state sintering yields samples exhibiting strong ferromagnetic hysteresis loops (MHLs), and the superconducting contribution is only visible after subtracting MHLs from above T_c. Due to the complicated phase diagram, the samples are a mixture of several phases, the superconducting β-FeSe, and the non-superconducting δ-FeSe and γ-FeSe. Furthermore, antiferromagnetic Fe_7Se_8 and ferromagnetic α-Fe may be contained, depending directly on the Se loss during the sintering process. Here, we show MHLs measured up to ±7 T and determine the magnetic characteristics, together with the amount of superconductivity determined from $M(T)$ measurements. We also performed a thorough analysis of the microstructures in order to establish a relation between microstructure and the resulting sample properties.

I. INTRODUCTION

The member of the iron-based superconductor (IBS) family with the simplest composition is FeSe ("11").[1,2] This material is not only interesting from the basic physics point of view,[3–5] but also for applications as the grain boundaries (GBs) may not be not obstacles as for the cuprate 123-HTSc,[6] and the main properties are like other high-temperature superconductors (HTSc), that is, high upper critical fields H_{c2}, high current densities j_c, and not being prone to flux jumps. Most importantly, the material is free of rare-earths and toxic elements.[7,8] Thus, it is interesting to use FeSe for metal-sheathed tapes,[9,10] but also for bulk applications like superconducting trapped field (TF) magnets.[11]

Now, many problems for the sample preparation appear due to the relatively complicated phase diagram of FeSe.[12–15] It was found that the composition $Fe_1Se_{1-\delta}$ is extremely sensitive to the correct stoichiometry.[14,15] All this makes the preparation of single crystals very difficult,[16] and the preparation of bulk, polycrystalline samples required for TF magnets is even more complicated. This was demonstrated by Diko *et al.*[17] using optical polarization

microscopy together with x-ray data. Furthermore, antiferromagnetic (AF) Fe_7Se_8 and ferromagnetic (FM) α-Fe particles may be contained, depending directly on the Se loss during the sintering process.

Thus, the preparation route to achieve good samples for applications must consider all the phase relations, and furthermore, recent results[18] have demonstrated that the critical currents obtained by the simple solid-state sintering are similar to that of the direct competitor, MgB_2, without additional flux pinning sites, but not yet sufficient for most bulk applications.

So, it is strongly required to learn more about the microstructures achieved in the sintering processes to devise a better suited preparation technique. In the present contribution, we employ optical and electron microscopy to gain a better understanding how the samples prepared by solid-state sintering are composed. The other important issue is how the presence of the secondary magnetic phases affect the superconducting properties.

II. EXPERIMENTAL PROCEDURE

Polycrystalline FeSe samples were prepared by solid-state sintering, starting from commercially available metallic Fe (99.9% purity) and Se (99.5% purity) powders. The powders were mixed together by ball-milling under Ar atmosphere. The resulting powder mixture was then pressed into pellets (5 mm diameter, 2 mm thick, 0.3 g) using uniaxial pressure of 10 MPa. The pellet was wrapped in Ta foil[19] and sealed into an evacuated quartz tube. The samples were then heated up to 700 °C with a rate of 50 °C/h and held there for 1 h. Then, the temperature was reduced to 400 °C in 30 min and maintained there for 40 h to enable the growth of the β-FeSe phase. Finally, the quartz tube with the sample was air-quenched to reach room temperature in about 5 min to avoid a low-temperature phase transformation.[14] To find the optimum conditions for our furnace system, the Se content δ was varied between 0.9 and 1.2. All products were checked using x-ray diffraction (XRD) in a powder diffractometer (Rigaku Ultima IV), using Cu-K_α radiation. Quantitative analysis was performed with the software Match! for Rietveld refinements. Typical XRD data are given in the supplementary material. For microscopy, the sample surfaces were mechanically polished using silicon carbide papers and diamond paste with alcohol as lubricant[20] For magnetometry, small samples (~1.5 × 1 × 0.7 mm^3) were cut from the big pellets. For resistance measurements, small bars (5 × 1 × 1 mm^3) were prepared, and the contacts were fixed with silver paint, ensuring about 3.5 mm distance between the voltage pads. The magnetic characterization measurements were performed using SQUID magnetometry (Quantum Design MPMS3) and the magneto-resistance characteristics were recorded using an Oxford Instruments 10/12 T Teslatron system with λ-plate. Polarization images were taken using a Zeiss Microplan system. Electron backscatter diffraction (EBSD) was performed employing a Zeiss Sigma VP microscope operating at 20 kV with Oxford Instruments EBSD detector and TSL analysis. The working distance was chosen to be 17 mm, the stepsize was 160 nm.

III. RESULTS AND DISCUSSION

Figure 1(a) presents magnetization hysteresis loops (MHLs) of a FeSe (initial composition Fe:Se=1:1.05) sample, taken at 4.2 K (■) and 20 K (●). The 20 K-loop is clearly above the superconducting region and shows ferromagnetic behavior with a small hysteresis. The 4.2 K-loop presents a combination of a ferromagnetic with a superconducting signal. At high fields above 6 T, both loops are nearly identical, but around zero field, the superconducting contribution (zero-field peak) is obvious. In (b), the simple subtraction of both loops is shown. The resulting MHL is asymmetric, which may stem from the polycrystalline character. However, the simple subtraction assumes that the two contributions are fully independent from each other. Measuring a large number of such MHLs demonstrated that this is not the case. This effect of the interaction of the magnetic and superconducting contributions will need to be investigated in more detail, determining the Meissner currents.

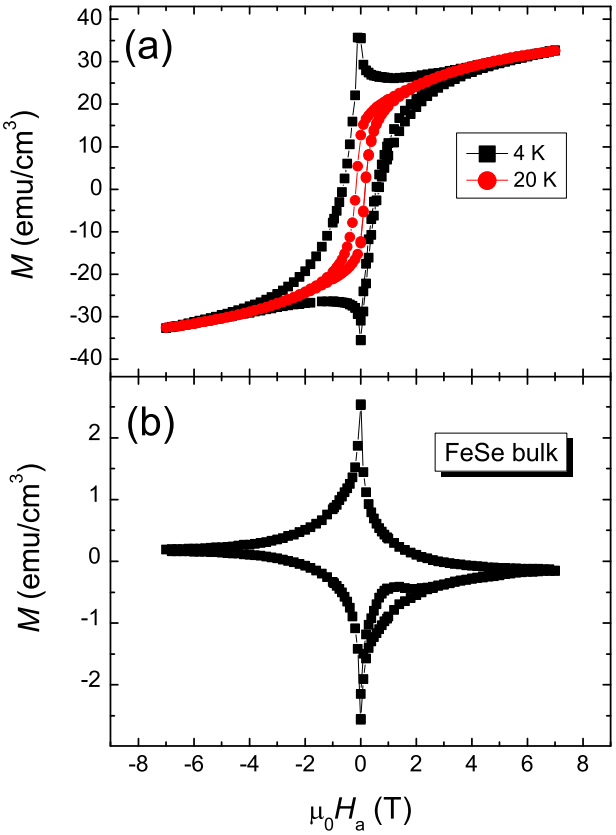

FIG. 1. (a) Magnetization hysteresis loops (MHLs) of a polycrystalline FeSe (initial composition Fe:Se=1:1.05) sample at 4.2 K (■) and 20 K (●). (b) Superconducting hysteresis loop after simple subtraction.

Figure 2 shows a plot of the magnetization (in units of μ_B/formula unit) as function of δ, the Se content in the formula $Fe_1Se_{1-\delta}$, following Williams *et al.*[15] In this way, it becomes possible to establish a relation between the prevailing magnetism and the Se content in the sample. The β-FeSe phase is non-magnetic, Fe_7Se_8 is antiferromagnetic,[21] and especially, eventually unreacted (due to Se loss) α-iron is ferromagnetic. Furthermore, we must note that the remaining high-temperature phase δ-FeSe (space group $P6_3/mmc$,

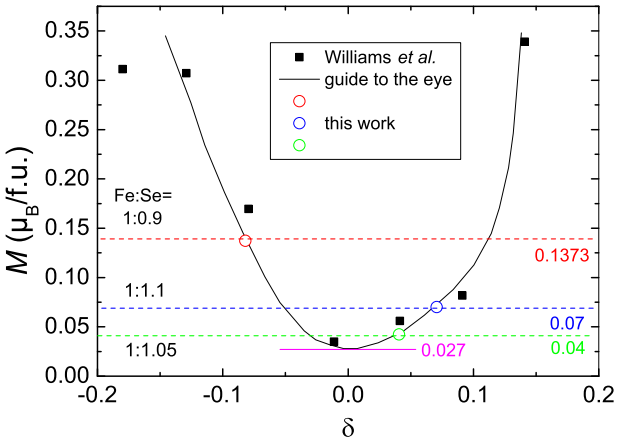

FIG. 2. Magnetization as function of the Se deficiency δ (T = 150 K, up to 9 T applied field). The solid line is a guide to the eye. The symbols (■) are the data of Ref. 15, the open symbols are the present work. The dashed lines give the saturation magnetization of our samples together with the precursor composition.

NiAs-type), which may be present in the samples, gives a background magnetization of 0.012 μ_B/f.u.,[22] which cannot be avoided as the conversion from δ-FeSe to β-FeSe cannot be complete.[17] The minimum of the curve in Fig. 2 is found, however, at 0.027 μ_B/f.u., which implies that there is an additional FM contribution, which may be α-Fe. This was not commented in Ref. 15. In our case, the minimum magnetization was 0.04 μ_B/f.u., and the corresponding x-ray results let us conclude that this point is on the side $\delta > 0$. Thus, the stoichiometry of Se in the starting mixture is crucial: If there is too much Se present in the sample, AF-Fe_7Se_8 will form, and if the Se loss is too high, unreacted FM α-iron will be found in the sample. The XRD analysis obtained via Match! gives 74.2 vol.-% β-FeSe and 25.8 vol.-% δ-FeSe for the sample Fe:Se=1:1.2, and 85.2 vol.-% β-FeSe and 14.8 vol.-% δ-FeSe for the sample Fe:Se=1:1.2, with the other phases treated as minor contribution. As the resulting particles or grains are in the nanometer range, it is difficult for common XRD to detect these contributions. Additionally, most of the peaks in the XRD diagram overlap each other, so it is not trivial to distinguish these phases. One possibility to obtain this information are the peaks at $2\Theta = 44.73^\circ$ (α-Fe) and 50° (Fe_7Se_8), which may enable to judge if δ is positive or negative. Thus, we decided to run EBSD to obtain a spatially resolved information about the phase distribution in our samples.

Figure 3 presents a polarization image, revealing twin patterns in the FeSe grains. (b) gives a SEM image, showing the FeSe grains (platelet-like shape) and the remaining pores in the sample. The density of the present samples is about 65% of the theoretical value.

Figure 4 shows the EBSD results on the polycrystalline FeSe sample (Fe:Se=1:1.05). Image (a) is a gray-scale image quality map of the sample section ($82 \times 62\ \mu m^2$) studied, which resembles an SEM image, but in EBSD condition with 70° incline. Image (b) presents the phase mapping: The light blue color indicates the superconducting β-FeSe phase, pink stands for α-iron and blue for Fe_7Se_8. Here it is interesting to note that both magnetic phases appear together inbetween the β-FeSe grains. The overall amounts detected by

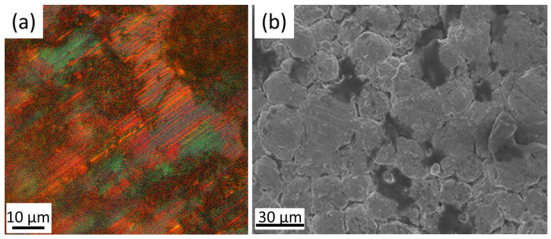

FIG. 3. (a) Polarization image of a polycrystalline FeSe (Fe:Se=1:1.05) sample, (b) SEM image.

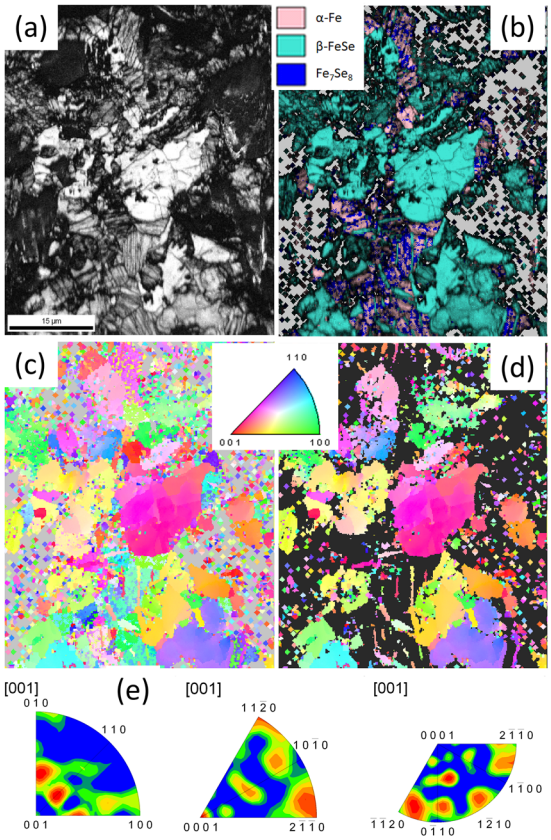

FIG. 4. EBSD analysis results on the sample Fe:Se=1:1.05. (a) Image quality map, (b) phase map, (c) IPF map for all phases together, (d) IPF map for β-FeSe separately, and (e) the inverse pole figures in [001]-direction for β-FeSe (left), α-Fe (middle) and Fe_7Se_8 (right).

EBSD are 54.4% β-FeSe, 17.4% α-Fe and 10.5% Fe_7Se_8. The remainder are pores, and non-indexed points including γ- and δ-FeSe. Note that these are data within the given surface. Therefore, this composition may vary with position. The dominating phase is always β-FeSe, and thus, purely superconducting paths exist in the sample. Image (c) presents an inverse pole figure (IPF) map in [001]-direction (i.e., perpendicular to the sample surface), showing the crystallographic orientation of all phases together, and (d)

gives the orientation of the β-FeSe grains separately. The measured Kikuchi patterns were indexed as β-FeSe (JCPDS file 030533, tetragonal, space group P4/nmm [129], PbO-type), α-iron (bcc) and Fe_7Se_8 (triclinic, space group $P3_121$). The color codes for the grain orientations are given in the stereographic triangles below the maps. Finally, (e) shows the inverse pole figures in [001]-direction for β-FeSe, α-Fe and Fe_7Se_8. From these maps, we see that the β-FeSe grains are not randomly oriented, but shows some distinct maxima. Furthermore, there is a needle-like arrangement of the grains with several intergrowths and other phases embedded within them. The strong orientation deviation leads to many high-angle grain boundaries, which are obstacles to the current flow even if the grain coupling in FeSe should be much better than in cuprate HTSc samples. According to Diko *et al.*,[17] the δ-FeSe formed in the first heating step undergoes a martensitic transformation below 457 °C, thus some longer dwell time below this temperature is required to allow the growth of β-FeSe. Also, due to this transformation, there are only some major directions of the β-FeSe as seen in the corresponding pole figure.

Having obtained these microstructure results, it is clear that in polycrystalline, bulk FeSe samples, there will always be some ferromagnetic contribution present due to remaining δ-FeSe, even if the extra phases α-Fe and Fe_7Se_8 can be avoided by properly selecting the starting composition. Thus, the superconducting properties of such samples will be always affected by this magnetic contribution. This is especially evident when extracting data for H_{c2}, where superconductivity vanishes completely. Such data can be obtained from magnetoresistance measurements with a criterion to define the first onset of superconductivty. Typically, a criterion of 99% R_N is applied,[25] where R_N is the normal state resistivity. $R(T, H_a)$-curves of our samples were already published,[26] so we focus here on the extracted data for H_{c2} (sample Fe:Se=1:1.05). Figure 5 shows

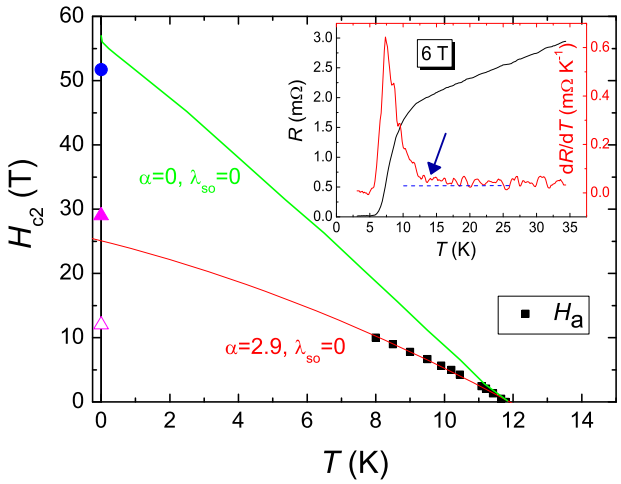

FIG. 5. $H_{c2}(T)$-data (■) obtained from resistance measurements on a FeSe sample (Fe:Se=1:1.05). The green (WHH) and red (with spin-paramagnetic effect) fits determine $H_{c2}(0)$. The inset presents $R(T)$ and dR/dT (6 T applied field). The arrow points to the onset of superconductivity at ~12 K. The data points at T = 0 K give the results of other works: $H_{c2}(0)$ = 12 T ($H_a \parallel c$, △), 29 T ($H_a \perp c$, ▲)[23] and 59 T (FIC analysis, ●).[24]

and the resulting data measured up to 10 T applied field. The onset of superconductivity takes place at ~12 K, whereas the main superconducting transition is found at 8.5 K (inset showing the resistive transition at 6 T applied field and its temperature derivative). The available field range is clearly not sufficient, so we need an extrapolation of the data towards 0 K. Commonly, the Werthamer-Helfand-Hohenberg (WHH) approach is employed for this purpose.[27] As shown by Cao *et al.*, this approach using the parameters α =0, λ_{so} =0 leads to a clear overestimation of H_{c2} in FeSe, yielding about 40 T for $H_a \parallel c$ on a signle crystalline sample. A similar value of ~ 57 T (●) was obtained from a fluctuation-induced conductivity study using our experimental data on polycrystalline FeSe.[24] When considering the spin-paramagnetic effect according to Ref. 28, then the fit using the parameters α =2.9 and λ_{so} = 0 gives H_{c2} = 25 T (randomly oriented polycrystal), which compares well to the result of Cao *et al.* with 12 T ($H \parallel c$, △) and 29 T ($H \perp c$, ▲). The $H_{c2}(0)$-values of FeSe deduced with the spin-paramagnetic contribution thus compare well with the data of the other IBS materials.[23,29]

These results for $H_{c2}(0)$ clearly demonstrate that the superconducting properties of FeSe are affected by the magnetism of Fe, and in the case of bulk, polycrystalline samples, the situation is even worse due the presence of AF or FM phases. Thus, the superconducting FeSe grains in such samples will always experience the local magnetic field created by the secondary phase particles.

IV. CONCLUSIONS

To conclude, we discussed the various phases appearing in superconducting bulk, polycrystalline β-FeSe samples intended for trapped field applications. By adjusting the Se-content in the precursor material to the given furnace setup, it is possible to minimize the magnetic contribution, but a fully non-magnetic sample cannot be obtained due to the presence of needle-like δ-FeSe, which is not converted to β-FeSe during the heat treatment. The resulting microstructure is thus very complicated including several phases. To obtain good quality, bulk FeSe samples, which are useful for trapped field applications, a treatment leading to a higher sample density is strongly required.

SUPPLEMENTARY MATERIAL

See supplementary material for the x-ray data of the FeSe samples.

ACKNOWLEDGMENTS

This work is part of the SUPERFOAM international project funded by ANR and DFG under the references ANR-17-CE05-0030 and DFG-ANR Ko2323-10, respectively. HO and SPKN gratefully acknowledge the support by JSPS KAKENHI, Grant Number JP16H6439. SPKN also wishes to thank JSPS for the fellowship (Grant No. P19354).

DATA AVAILABILITY

The data that support the findings of this study are available from the corresponding author upon reasonable request.

REFERENCES

[1] F.-C. Hsu, J.-Y. Luo, K.-W. Yeh, T.-K. Chen, T.-W. Huang, P. M. Wu, Y.-C. Lee, Y.-L. Huang, Y.-Y. Chu, D.-C. Yan, and M.-K. Wu, "Superconductivity in the PbO-type structure α-FeSe," Proc. Natl. Acad. Sci. **105**, 14262 (2008).

[2] Y. Mizoguchi and Y. Takano, "Review of Fe chalcogenides as the simplest Fe-based superconductor," J. Phys. Soc. Jpn. **79**, 102001 (2010).

[3] M. V. Sadovskii, "High-temperature superconductivity in iron-based layered compounds," Phys. Uspekhi **51**, 1201–1227 (2008).

[4] J. Pietosa, D. J. Gawryluk, R. Puzniak, A. Wisniewski, J. Fink-Finowicki, M. Kozlowski, and M. Berkowski, "Pressure-induced enhancement of the superconducting properties of single-crystalline $FeTe_{0.5}Se_{0.5}$," J. Phys. C: Condensed. Mat. **24**, 265701 (2012).

[5] J. H. J. Martiny, A. Kreisel, and B. M. Andersen, "Theoretical study of impurity-induced magnetism in FeSe," Phys. Rev. B **99**, 014509 (2019).

[6] T. Katase, Y. Ishimaru, A. Tsukamoto, H. Hiramatsu, T. Kamiya, K. Tanabe, and H. Hosono, "Advantageous grain boundaries in iron pnictide superconductors," Nature Comm. **2**, 409 (2011).

[7] H. Hosono, A. Yamamoto, H. Hiramatsu, and Y. Ma, "Recent advances in iron-based superconductors toward applications," Materials Today **21**, 278–302 (2018).

[8] Y. Ma, "Progress in wire fabrication of iron-based superconductors," Supercond. Sci. Technol. **25**, 113001 (2012).

[9] C. Dong, H. Huang, and Y. Ma, "Slow vortex creep induced by strong grain boundary pinning in advanced BA122 superconducting tapes," Chin. Phys. Lett. **36**, 067401 (2019).

[10] C. Yao and Y. Ma, "Recent breakthrough developemt in iron-based superconducting wires for practical applications," Supercond. Sci. Technol. **32**, 023002 (2019).

[11] J. D. Weiss, A. Yamamoto, A. A. Polyanskii, R. B. Richardson, D. C. Larbalestier, and E. E. Hellstrom, "Demonstration of an iron-pnictide bulk superconducting magnet capable of trapping over 1 T," Supercond. Sci. Technol. **28**, 112001 (2015).

[12] H. Okamoto, "The Fe–Se (iron-selenium) system," J. Phase Equilibria **12**, 383–389 (1991).

[13] E. Pomjakushina, K. Conder, V. Pomjakushin, M. Bendele, and R. Khasanov, "Synthesis, crystal structure, and chemical stability of the superconductor $FeSe_{1-x}$," Phys. Rev. B **80**, 024517 (2009).

[14] T. M. McQueen, Q. Huang, V. Ksenofontov, C. Felser, Q. Xu, H. Zandbergen, Y. S. Hor, J. Allred, A. J. Williams, D. Qu, J. Checkelsky, N. P. Ong, and R. J. Cava, "Extreme sensitivity of superconductivity to stoichiometry in $Fe_{1-\delta}Se$," Phys. Rev. B **79**, 014522 (2009).

[15] A. J. Williams, T. M. McQueen, and R. J. Cava, "The stoichiometry of FeSe," Solid State Commun. **149**, 1507–1509 (2009).

[16] S. Kasahara, T. Watashige, T. Hanaguri, Y. Kohsaka, T. Yamashita, Y. Shimoyama, Y. Mizukami, R. Endo, H. Ikeda, K. Aoyama, T. Terashima, S. Uji, T. Wolf, H. von Löhneysen, T. Shibauchi, and Y. Matsuda, "Field-induced superconducting phase of FeSe in the BCS-BEC cross-over," Proc. Nat. Acad. USA **111**, 16309–16313 (2014).

[17] P. Diko, V. Antal, V. Kavečansky, C. Yang, and I. Chen, "Microstructure and phase transformations in FeSe superconductor," Physica C **476**, 29–31 (2012).

[18] A. Koblischka-Veneva, M. R. Koblischka, K. Berger, Q. Nouailhetas, B. Douine, M. Muralidhar, and M. Murakami, "Comparison of temperature and field dependencies of the critical current densities of bulk YBCO, MgB_2, and iron-based superconductors," IEEE Trans. Appl. Supercond. **29**, 6801805 (2019).

[19] J.-C. Grivel, "A simple method for preparing superconducting FeSe pellets without sealing in evacuated silica tubes," Ceram. Int. **43**, 11474–11480 (2017).

[20] M. R. Koblischka and A. Koblischka-Veneva, "Application of the electron backscatter diffraction technique to ceramic materials," Phase Trans. **86**, 651–660 (2013).

[21] C. Boumford and A. H. Morrish, "Magnetic properties of the iron selenide Fe7Se8," Phys. Stat. Solidi (a) **22**, 435–444 (1974).

[22] Materials Project mp-1090, Dataset. https://doi.org/10.17188/1187442.

[23] R. X. Cao, J. Dong, Q. L. Wang, Y. J. Wang, C. Zhao, X. H. Zeng, D. A. Chareev, A. N. Vasiliev, B. Wu, and G. Wu, "Measurements of the superconducting anisotropy in FeSe with a resonance frequency technique," AIP Adv. **9**, 045220 (2019).

[24] M. R. Koblischka, Y. Slimani, A. Koblischka-Veneva, T. Karwoth, X. Zeng, E. Hannachi, and M. Murakami, "Excess conductivity analysis of polycrystalline FeSe samples with addition of Ag," Materials **13**, 5018 (2020).

[25] X. Zhu, H. Yang, L. Fang, G. Mu, and H.-H. Wen, "Upper critical field, Hall effect and magnetoresistance in the iron-based layered superconductor $LaFeAsO_{0.9}F_{0.1-\delta}$," Supercond. Sci. Technol. **21**, 105001 (2008).

[26] T. Karwoth, K. Furutani, M. R. Koblischka, X. L. Zeng, A. Wiederhold, M. Muralidhar, M. Murakami, and U. Hartmann, "Electrotransport and magnetic measurements on bulk FeSe superconductors," J. Phys.: Conf. Ser. **1054**, 012018 (2017).

[27] N. R. Werthamer, E. Helfand, and P. C. Hohenberg, "Temperature and purity dependence of the superconducting critical field, Hc2. III. Electron spin and spin-orbit effects," Phys. Rev. **147**, 295–302 (1966).

[28] G. Fuchs, S.-L. Drechsler, N. Kozlova, M. Bartkowiak, J. E. Hamann-Borrero, G. Behr, K. Nenkov, H.-H. Klauss, H. Maeter, A. Amato, H. Luetkens, A. Kwadrin, R. Khasanov, J. Freudenberger, A. Köhler, M. Knupfer, E. Arushanov, H. Rosner, B. Büchner, and L. Schultz, "Orbital and spin effects for the upper critical field in As-deficient disordered Fe pnictide superconductors," New J. Phys. **11**, 075007 (2009).

[29] Y. Sun, H. Ohnuma, S. Ayukawa, T. Noji, Y. Koike, T. Tamegai, and H. Kitano, "Achieving the depairing limit along the c-axis in $Fe_{1+\gamma}Te_{1-x}Se_x$ single crystals," Phys. Rev. B **101**, 134516 (2020).